

A 2-D transient multicomponent simulation model: Application to pipe wall corrosion

G. Naser, B.W. Karney*

Department of Civil Engineering, University of Toronto, Toronto, Canada

Received 14 February 2007; revised 14 April 2007; accepted 18 April 2007

Abstract

A transient multicomponent water quality (WQ) model of a distribution system is developed and then applied to the problem of predicting the concentration of corrosion-related chemicals released into a bare pipe system. The modeled reactions include dissolved oxygen (DO) which oxidizes iron (Fe) at the pipe wall to produce ferrous and hydroxide ions (Fe^{2+} and OH^-). These chemicals can then interact to produce substances like iron hydroxide, which ultimately deposits on the pipe wall. In this study, 1-D and 2-D simulation models are considered and the movement of each chemical is represented by the advection–diffusion–reaction equation (ADRE), which is coupled to the continuity and momentum equations for flow. A five-region turbulence model is used to represent cross-sectional variations and a combination of finite difference and characteristic methods are used to integrate the governing equations. The effects of key parameters (e.g., pH, initial DO concentration, and pipe diameter) are briefly explored and clearly show an increase in dissolved iron with increasing initial DO and pH, and in smaller pipes. The study highlights the influence of velocity profile on the diffusion of oxidants from the bulk flow to the pipe wall and thus underlines the importance of both the turbulence structure and pipe diameter to reactions in general and to corrosion in particular.

© 2007 International Association for Hydraulic Engineering and Research, Asia Pacific Division. Published by Elsevier B.V. All rights reserved.

Keywords: Transient flow; Multicomponent water quality model; Corrosion; Iron release; Oxidation–reduction reaction; Method of characteristics; Finite difference method

1. Introduction

The rapid expansion of urban areas is a global phenomena but one with particular importance to Asia. Urban populations are growing rapidly in China, India and many other areas, necessitating both large-scale construction of new urban areas and re-designing of deteriorated or inadequate systems. This expansion creates both social and infrastructure challenges since cities must be increased and in space and capacity to meet the growing demands for high quality water. This paper addresses one facet of this issue, focusing on the need to protect and support the people who use the potable water supply systems. By offering a more robust and comprehensive

formulation of the water quality transformations, engineers and officials can better protect public health and better understand system response.

Of particular interest is the general subject of this paper, namely the water interactions with aging infrastructure, and how chemical conditions evolve during transit. In particular, water quality (WQ) in a water distribution system (WDS) is transformed as a three-way interaction between the water itself, the hydraulic and chemical conditions during transport, and the nature of the confining space, particularly the pipe wall. The flow velocity is shown to be crucial in this regard, for it can not only significantly alter the rate of the reactions, but also influence the time available for reactions through the residence time. Interestingly, such WQ changes, as well as their numerical prediction, have been recognized in the literature as important for well over 100 years (De Mussy, 1849; Anon., 1878 in Kuch and Wagner, 1983).

* Corresponding author.

E-mail addresses: gnaser@ecf.utoronto.ca (G. Naser), karney@ecf.utoronto.ca (B.W. Karney).

Nomenclature

A	pipe cross-sectional area (L^2)	$S(C_k)$	source/sink term of the k th chemical ion in bulk flow
C_k	concentration of k th chemical (ML^{-3})	SC_k	turbulent Schmidt number for k th chemical ion
\bar{C}_k	cross-sectional averaged concentration of k th chemical (ML^{-3})	S_t	source/sink term at pipe wall in transport equation
c	turbulent fluctuation of a chemical's concentration (ML^{-3})	S_{to_2}	sink term at pipe wall for dissolved oxygen
C_{O_2}	dissolved oxygen concentration (ML^{-3})	S_{toH^-}	source term at pipe wall for hydroxyl ion
C_{OH^-}	hydroxyl ion concentration (ML^{-3})	$S_{tFe^{2+}}$	source term at pipe wall for ferrous ion
$C_{Fe^{2+}}$	ferrous ion concentration (ML^{-3})	t	time (T)
C_r	Courant number	T_{tf}	transient flow time scale (T)
C_o	initial concentration for chlorine (ML^{-3})	T_{wq}	WQ time scale (T)
C_{k_o}	initial concentration for k th chemical ion (ML^{-3})	U	longitudinal component of time-averaged velocity (LT^{-1})
$C_{k_{in}}$	concentration of k th chemical ion at inlet section (ML^{-3})	U^*	shear velocity (LT^{-1})
C_b, C_m	parameters in five-region turbulence model	u	turbulence velocity fluctuations in longitudinal direction (LT^{-1})
C_c, C_{c2}, C_{c3}	parameters in five-region turbulence model	V	radial component of the time-averaged velocity (LT^{-1})
C_{u1}, C_{u2}, C_{u3}	parameters in method of characteristics discretization	v	turbulence velocity fluctuations in the radial direction (LT^{-1})
C_{m1}, C_{m2}	parameters in method of characteristics discretization	x	distance along the centerline of the pipe (L)
D	pipe diameter (L)	y	distance from pipe wall (L)
E_v	head loss coefficient of valve ($L^{2.5} T^{-1}$)	y^*	shear-velocity-based distance from pipe wall (L)
f	Darcy–Weisbach friction factor		
g	acceleration due to gravity (LT^{-2})	<i>Greek notation</i>	
H	Piezometric head (L)	β	parameters in five-region turbulence model
i, j	subscripts denotes the position of the node in longitudinal and radial directions	Γ	turbulent diffusion coefficient ($L^2 T^{-1}$)
J_x, J_r	mass flux in longitudinal and radial directions ($ML^{-2} T^{-1}$)	Γ_m	molecular diffusion coefficient ($L^2 T^{-1}$)
k	subscript indicates the chemical constituent	κ	Von-Karman parameter in five-region turbulence model
K_r	chemical reaction rate coefficient	ρ	fluid specific mass (ML^{-3})
K_{eq}	activity equilibrium constant of a chemical reaction	τ	turbulent shear stress ($ML^{-1} T^{-2}$)
L	pipe length (L)	τ_w	turbulent wall shear stress ($ML^{-1} T^{-2}$)
m	radial flow per unit length ($L^2 T^{-1}$)	ν_t	turbulent kinematic viscosity ($L^2 T^{-1}$)
n	superscript denotes the time level	ν	molecular kinematic viscosity ($L^2 T^{-1}$)
n_1, n_2, n_3	orders of reactions' kinetics	ΔG^o	standard Gibbs free energy change ($ML^2 T^{-3}$)
N_x	number of reaches in longitudinal direction	Δt	time step in numerical discretization (T)
N_r	number of cylinders in radial direction	Δt_{tf}	time step for transient flow analysis (T)
R	pipe radius (L)	Δt_{wq}	time step for WQ analysis (T)
r	distance along radial direction or radial coordinate axis (L)	Δx	pipe reach length in numerical discretization (L)
		Δr	increase in radius of cylinders in numerical discretization

Given the importance of WQ, it is not surprising that many models have been created to predict the chemical and hydraulic properties of delivered water. In general, there are five groups of WDS simulation models commonly discussed in the literature. These are briefly summarized here to position where within this spectrum the current research fits.

- Steady-state models, now rarely used due to their limitations, are based on the time-invariant assumptions for both hydraulic conditions and the concentration of chemicals (Wood, 1980; Clark et al., 1988; Boulos et al., 1993).
- 1-D quasi-steady or extended period models allow for limited unsteadiness in flow and in chemical concentration. Such models, which typically trace the fate of a single chemical constituent, seldom use sophisticated turbulence or diffusion concepts, and explicitly ignore inertia and compressibility effects (Liou and Kroon, 1987; Grayman et al., 1988; Rossman et al., 1993; Boulos et al., 1995; Rossman and Boulos, 1996). Nevertheless, these models comprise the basic structure of the most commonly used WQ software (e.g., EPANET and several other related commercial software packages).

- More complete transient (water hammer) models assume temporal variations for both flow and concentration variables (Fernandes and Karney, 2004). Such models account for the sometimes important role of water inertia and compressibility but are typically 1-D in nature, usually using steady-state friction formulas (e.g., Darcy–Weisbach equation) to determine the shear stress and Taylor’s model to estimate diffusion.
- Considering steady conditions for hydraulics, a quasi 2-D model studies WQ through a 2-D unsteady transport model for the chlorine concentration (Ozdemir and Ger, 1998, 1999). Various other 2-D models have been created but a few have been adapted to include constituent modeling, rather than being concerned with water hammer phenomena and its resolution.
- Computational Fluid Dynamics (CFD) tools are another group of simulation models. Using direct numerical simulation and large eddy simulation approaches, Waanders et al. (2005) verify that although the 3-D CFD tools can potentially characterize fluid flow and chemical mixing in highly turbulent flows with complex boundaries, such modeling is unnecessary for practical purposes. Moreover, even for nominally steady flows such simulations are computationally demanding and are often prohibitively expensive for the entire WDS.

Considering simplicity and accuracy as twin goal of a simulation model, the first two groups of models described above are viewed here as too simple and inaccurate to capture the full range of disturbances that characterize realistic water distribution system events. By contrast, the last group of models, while potentially slightly more accurate, are still computationally impractical for the range of routine analysis and decision making that is demanded in practice. Thus, the current paper considers that the set of models of the third and fourth groups are an appropriate compromise, thus justifying further exploration here. Such models are expected to be reasonably accurate (they consider a more realistic set of conditions and changes in flow state and chemical concentration), yet are sufficiently efficient computationally to be economical.

However, there is another dimension that deserves brief consideration. Historical models, whatever their classification, have considered the fate and transport of only single chemical species simultaneously. Yet WQ can actually degrade through a variety of chemical/biological reactions taking place between a variety of chemical species and with the pipe wall (Tangara, 2004). In summary, then, the current research proposes a more realistic multicomponent approach in three different ways: considering reacting and interacting chemical reactions, unsteady transient events, and also through permitting cross-sectional effects.

2. Specifics and context of the current model

So pipe corrosion is studied here as a typical multicomponent WQ application. In this preliminary study, both 1-D and

2-D transient models are considered by coupling a mass transport ADRE for individual chemical compounds with a comprehensive model for flow. In this way, using the modified Vardy–Hwang model, a 2-D hydraulic model for transient flow was further coupled with a 2-D ADRE for the concentration of individual chemical ions released into the water. The decay/growth of several ionic species is studied with a first order reaction term. This coupling of the hydraulic and ADRE is accomplished by introducing two different numerical schemes; one for the mass transport and the other for the system hydraulics. Specifically, a finite difference method (FDM) is used to numerically integrate ADRE and the method of characteristics (MOC) is used to integrate the continuity and momentum equations. Considering different mechanisms responsible for turbulent damping within a pipe section, the standard five-region turbulence model is used to capture the velocity fluctuations while limiting the computational burden. Finally, the numerical results of the proposed 2-D model are compared with those from a transient 1-D model.

Although the intent of this research is not to thoroughly describe the corrosion phenomenon from either a chemical or physical point of view, the goal is to highlight key hydraulic and chemical interactions influencing WQ transformations. Pipe corrosion is useful in this regard both as a representative WQ example and an important multicomponent system in its own right. Yet, it is fair to note that the process of internal corrosion occurs over the life-time of a pipe whereas a transient event is usually a short term disturbance. Thus, there is an apparent mismatch in the time scale between that of transient flow (typically seconds and minutes) and that of the corrosion kinetics (typically years or decades). However, many transient-induced WQ changes are important and worthy of study. Examples of this include both discoloration events and situations in which deposited material may be rapidly re-suspended into the bulk flow. Indeed, there is a potential that transient phenomena could be to corrosion in pipes as floods are to rivers – i.e., that both are relatively rare, rapid and potentially dramatic events. Moreover, it is emphasized that there is nothing (except perhaps execution time) about the proposed 2-D transient model that precludes its use for steady flow phenomena. As is so often the case, it is primarily the creativity of the analyst that limits or extends the power of a broad and well-conceived modeling construct.

3. Mathematical model

3.1. Hydraulic model

The current mathematical representation of the turbulent flow begins with Vardy and Hwang (1991) model, a model that discretizes the pipe into several hollow concentric cylinders allowing the lateral flow between adjacent cylinders. Consequently, the hydraulic model was expressed as a quasi 2-D representation for the longitudinal continuity and the momentum equations. Zhao and Ghidaoui (2003) modified Vardy and Hwang model by decoupling the original flow equations into two sets; one for piezometric head and radial flux and the other

for axial velocity. As they argued, the application of the modified scheme to the realistic systems lowers execution time by two orders of magnitude. This smaller execution time makes the modified quasi 2-D model more efficient in practice. More details of the hydraulic model are found in Zhao and Ghidaoui (2003).

3.2. Water quality model

A clear understanding of the transport of chemical constituents including DO, OH^- , and Fe^{2+} from the bulk flow to the pipe wall is an important prerequisite to the corrosion and the WQ modeling. A key mechanism responsible for WQ changes is the reaction between the chemical compounds flowing with the water and the pipe wall material. In general, the rates of this mechanism depend upon many factors including flow conditions, the material and age of the pipe, and the residual concentration of the chemical compounds within the water. Using the mass conservation law for the constituent, the following second-order parabolic partial differential equation in cylindrical coordinate system represents the unsteady advection–diffusion–reaction equation (ADRE) for the k th chemical concentration:

$$\frac{\partial C_k}{\partial t} + U \frac{\partial C_k}{\partial x} + V \frac{\partial C_k}{\partial r} = \frac{1}{r} \frac{\partial}{\partial r} (r J_r) + \frac{\partial J_x}{\partial x} \pm S(C_k) \quad (1)$$

in which r and x , are coordinates in cylindrical system; U and V are longitudinal and radial velocity components; C is the chemical concentration at point (x, r) and time t ; $S(C)$ is the source/sink term defining the production/consumption of the k th chemical in the bulk flow during the corrosion process, J_x and J_r are the mass flux in longitudinal and radial directions, respectively. The subscript k denotes the chemical constituents in the water (i.e., DO, OH^- , and Fe^{2+}). The ADREs of each chemical are coupled via the source/sink terms.

The last two terms on the left side of Eq. (1) represent the advection of chemicals throughout the pipe by the bulk flow and the first two terms on the right side account for the diffusion of the chemicals toward the pipe wall (radial direction) and along the pipe (longitudinal direction). The last term in Eq. (1) represents the decay/growth of the chemicals due to their reactions with other substances (organic and inorganic matters) in the bulk flow. For the 1-D case, the radial advective term (V) in left side and radial flux term (J_r) in right side of Eq. (1) must be eliminated.

As Rodi (1993) argued, the turbulent mass transport can logically be related to the gradient of the transported quantity (chemical concentration in this study) in direct analogy to the turbulent momentum transport. Hence:

$$-\overline{uc_k} = J_{x_k} = (\Gamma_k + D_{m_k}) \frac{\partial C_k}{\partial x} \quad (2)$$

$$-\overline{vc_k} = J_{r_k} = (\Gamma_k + D_{m_k}) \frac{\partial C_k}{\partial r} \quad (3)$$

in which c_k is the fluctuation of concentration of the k th ion and Γ and D_m are, respectively, the turbulent and molecular diffusivity coefficients. Using the Reynolds analogy between the mass transport and the momentum transport, Rodi obtained the turbulent diffusivity coefficient from the eddy diffusivity concept through the relation:

$$\Gamma_k = \nu_t / SC_k \quad (4)$$

where SC_k is the dimensionless turbulent Schmidt number for the k th chemical and ν_t is the turbulent viscosity coefficient. The turbulent Schmidt number has only small variations across any flow and also from flow to flow. Consequently, like many other models the turbulent Schmidt number was considered constant and equal to unity throughout this study.

3.3. Chemical reactions at pipe wall

Corrosion attacks the metal surface by electron transfer reactions. In these reactions, the metal is oxidized at the anode generating electrons and positive ferrous ions (Fe^{2+}). The electrons migrate through the internal circuit (pipe wall) to the cathode. The acceptors at the cathode (i.e., DO or other chemicals) absorb the electrons through chemical reduction reactions, producing negative hydroxide ions (OH^-). Due to the concentration gradient and in order to balance the charge, the positive ions migrate from anode to cathode and similarly the negative ions migrate from cathode to anode. In this way, the ferrous ion reacts with hydroxide ion to produce iron hydroxide, which deposits on the pipe wall creating tubercles. In general, the study of corrosion study is based on two types of the chemical reactions, the so-called primary and secondary reactions.

3.3.1. Primary reactions

These are the direct oxidation–reduction reactions occurring at the anode and cathode as follows:

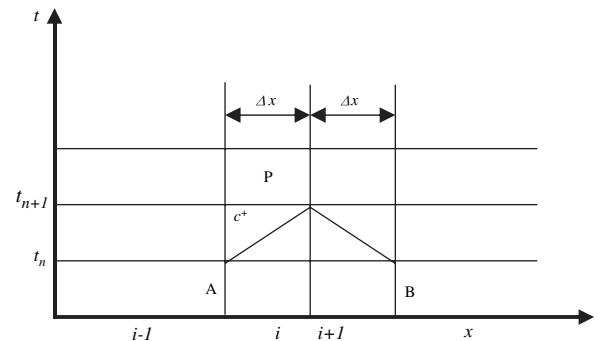


Fig. 1. Longitudinal discretization of pipe in MOC.

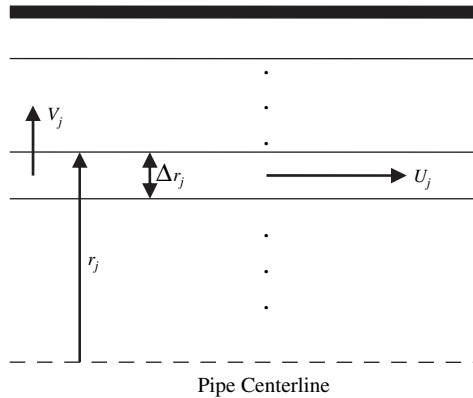
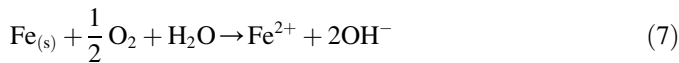


Fig. 2. Radial discretization of pipe into concentric cylinders.

According to Eq. (6) the hydroxide ion is produced at the cathode, which tends to increase the pH of the solution. The primary reactions (5) and (6) can be summarized as follows:



The standard Gibbs free energy change for Eq. (7) is estimated as $\Delta G^0 = -78.0$ kcal (Benfield et al., 1982), with the negative value indicating the spontaneous conversion of reactants to products at standard condition. Chemical equilibrium is determined by:

$$K_{\text{eq}} = \frac{C_{\text{Fe}^{2+}} C_{\text{OH}^-}^2}{C_{\text{O}_2}^{1/2}} \quad (8)$$

in which K_{eq} (mole^{1.5}) is the activity equilibrium constant for the chemical reaction, which is approximately 10^{57} at standard condition (Benfield et al., 1982).

3.3.2. Secondary reactions

The ferrous iron released into the water by Eq. (5) reacts with the hydroxide ions through the secondary reactions, thus producing the ferrous hydroxide.



The ferrous hydroxide precipitates on the pipe wall creating layers of tubercles around the anodic areas. These layers protect the pipe wall and limit further corrosion.

The current study is focused only on the primary reactions. In such an environment, the rate of change of the chemical ions due to Eqs. (5) and (6) is governed by:

$$-2 \frac{\partial C_{\text{O}_2}}{\partial t} = \frac{\partial C_{\text{Fe}^{2+}}}{\partial t} = \frac{1}{2} \frac{\partial C_{\text{OH}^-}}{\partial t} = K_r C_{\text{O}_2}^{n_1} C_{\text{OH}^-}^{n_2} C_{\text{Fe}^{2+}}^{n_3} \quad (10)$$

in which K_r is the reaction rate coefficient, n_1, n_2, n_3 are the order of kinetics, C_{O_2} , C_{OH^-} and $C_{\text{Fe}^{2+}}$ are the concentrations of DO, OH^- , and Fe^{2+} ions, respectively. In general, the order of kinetics and the rate of any chemical reaction are not determined by the stoichiometry of the reaction, but are evaluated experimentally. However, due to their simplicity and relatively accurate/reasonable results, zeroth or first order kinetics have been traditionally considered in the literature for most chemical reactions. A first order model is adopted here with respect to oxygen and hydroxide and a pseudo-first order with respect to iron.

3.3.3. Turbulence model

The Reynolds shear stress terms in the hydraulic model and the turbulent diffusivity of each constituent within the flow could readily be calculated using the eddy viscosity and eddy diffusivity concepts. In principle, the simulation model of this study can be used with any prescribed turbulence model based on the eddy viscosity concept. However, to overcome the complexity in the determination of the turbulent shear stresses and to reduce the computational burden, the standard five-region turbulence model, initially proposed by Kita et al. (1975), was used to model velocity fluctuations. This approach is justified by the different mechanisms responsible for damping the turbulence, with molecular viscosity being dominant in the region near the pipe wall (viscous sub-layer) and eddy viscosity being dominant in the core region. The five-region turbulence model is specified in detail in Kita et al. (1975).

4. Numerical solution of the governing equations

A numerical model should be consistent and stable so that it is convergent; but it should also have the desirable human attributes of being easy to use, modify, and implement, and it should be efficient in terms of computational time and memory requirements (Abbott and Minns, 1998). The challenge of WQ simulation arises from the need to couple the parabolic nature of the ADRE to the parabolic nature of the hydraulic equations. In this study, ADRE is integrated by the FDM



Fig. 3. Schematic of the pipe system for the case study.

and the flow equations by the method of characteristics (MOC).

4.1. Method of characteristics

Using the MOC and following Zhao and Ghidaoui (2003), the hyperbolic partial differential equations (PDEs) of flow hydraulics are converted into a pair of ordinary differential equations (ODEs) along the positive and negative characteristic lines and then integrated numerically. The longitudinal and radial discretizations of the pipe flow domain are shown in Figs. 1 and 2, respectively. More details are given in Zhao and Ghidaoui (2003).

4.2. Finite difference method

An FDM approach, namely the Alternating Direction Implicit (ADI) approach, was used here to integrate numerically Eq. (1). As Ferziger (1981) argued, the ADI scheme provides an efficient numerical solution to the parabolic differential equations using tridiagonal matrices. Knowing the concentrations at the previous time level (n) and using the finite difference scheme in both the radial and longitudinal directions, the discretization of Eq. (1) for the next time level ($n + 1$) is divided into two half steps.

For the first step, the technique is implicit in the radial direction but explicit in the longitudinal direction, providing the following set of tridiagonal equations for the unknown k th chemical concentrations at each node at the intermediate time level $n + 1/2$:

$$A_{k1} C_{k_{i,j+1}}^{n+1/2} + B_{k1} C_{k_{i,j}}^{n+1/2} + E_{k1} C_{k_{i,j-1}}^{n+1/2} = F_{k1} \quad (11)$$

For the second half step, the scheme is explicit in the radial direction but implicit in the longitudinal direction, providing another set of tridiagonal matrices for the unknown k th chemical concentrations at each node at the time level $n + 1$ as follows:

$$A_{k2} C_{k_{i+1,j}}^{n+1} + B_{k2} C_{k_{i,j}}^{n+1} + E_{k2} C_{k_{i-1,j}}^{n+1} = F_{k2} \quad (12)$$

This cycle repeats over the whole simulation period. Overall, the solution of these two sets of equations provides the unknown concentrations at each node for the corresponding time level. The subscript i denotes the position of the node in the longitudinal direction and the subscript j denotes the position of the node in the radial direction, while the superscript n denotes the time level. The coefficients in Eqs. (11) and (12) are given in the Appendix.

4.3. Boundary and initial conditions

The boundary condition at the upstream end is considered as a fixed concentration node and the water in the pipe initially has no iron. The pipe wall condition is modeled as:

$$\Gamma \frac{\partial C_k}{\partial r} \Big|_{x,r=R}^t = S_{tk} \quad (13)$$

that must hold at any point on the pipe wall ($x, r = R$) at any time (t). The source/sink terms (S_{tk}) for each chemical compound in Eq. (13) are due to the chemical reactions at the pipe wall, which using Eq. (10) can be expressed as:

$$S_{t_{Fe^{2+}}} = K_1 C_{O_2}^{n1} C_{OH^-}^{n2} C_{Fe^{2+}}^{n3} = \frac{1}{2} S_{t_{OH^-}} = -2S_{t_{O_2}} \quad (14)$$

The ADREs of each chemical are coupled via Eq. (14). An explicit numerical approach was used here to numerically integrate the ADREs (1). More accurate and numerically stable results can be obtained through an implicit approach, but at greater computational cost. The pipe centerline is taken as a no-flux (symmetry) boundary for all chemical constituents:

$$\frac{\partial C_k}{\partial r} \Big|_{x,r=0}^t = 0 \quad (15)$$

5. Illustration using system start-up

In order to explore in a preliminary way the capabilities of the proposed 2-D numerical model in simulating a multicomponent WQ problem, a system consisting of a pipeline, which connects two constant-head reservoirs, is used (Fig. 3). The pipeline is 1000 m long, 1128.4 mm in diameter, its Darcy–Weisbach friction factor is 0.05 and the wave speed is 1000 m/s. The water in the reservoirs is at the elevation of 200 m and 180 m for the upstream and downstream reservoirs, respectively. The final steady-state flow rate (with the valve fully open) is 1600 l/s. The system has no flow initially and the valve is fully closed. Then, the valve is suddenly opened to introduce a transient state, during which clean water (with no iron concentration) with pH = 7 and 5 mg/l of DO is continuously supplied at the upstream end. The initial steady-state conditions for pH, DO, and iron concentrations are set as 7, 5 mg/l, and 0 mg/l, throughout the flow domain, respectively. To facilitate the comparison between the results of the 1-D and 2-D models, the local concentration of the 2-D simulation is averaged over the pipe cross-section.

6. 1-D and 2-D models results

The 1-D and 2-D system responses for the chemical concentrations along the pipeline are given in Figs. 4–8. Overall, following the opening of the valve, a pressure and flow disturbance is created that persists until a new steady state is achieved. However, compressibility and inertia cause an overshoot of the final values and a sequence of oscillations. It takes approximately 20 s for the system to reach the 1600 l/s steady-state discharge.

Fig. 4a–c shows both 1-D and 2-D simulation results for the consumption of DO, increase in pH, and ferrous iron release into the bulk flow, 5 min and 1 h after start-up. Overall, there

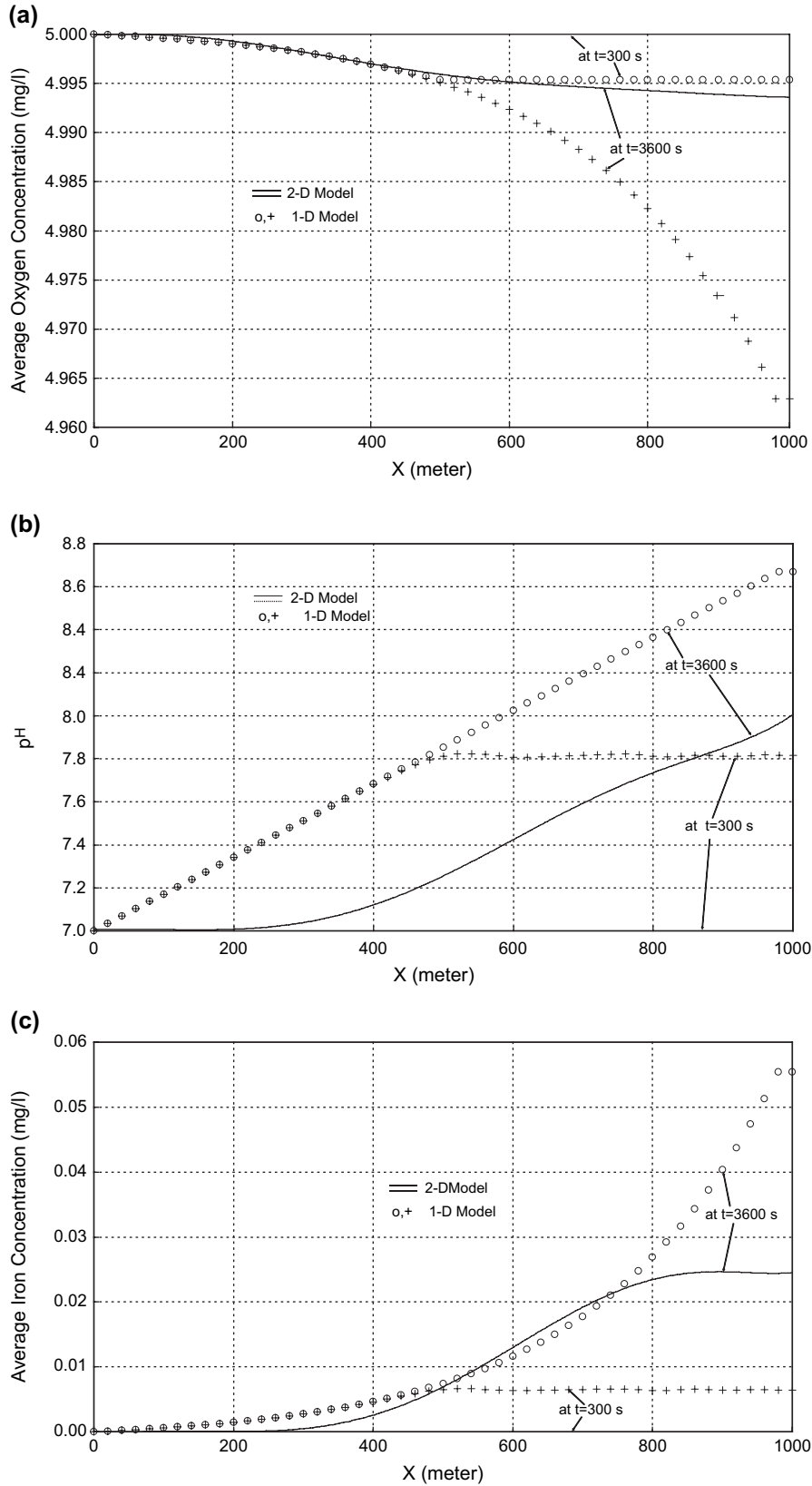


Fig. 4. Concentration along the pipe; (a) DO concentration, (b) pH, (c) iron release.

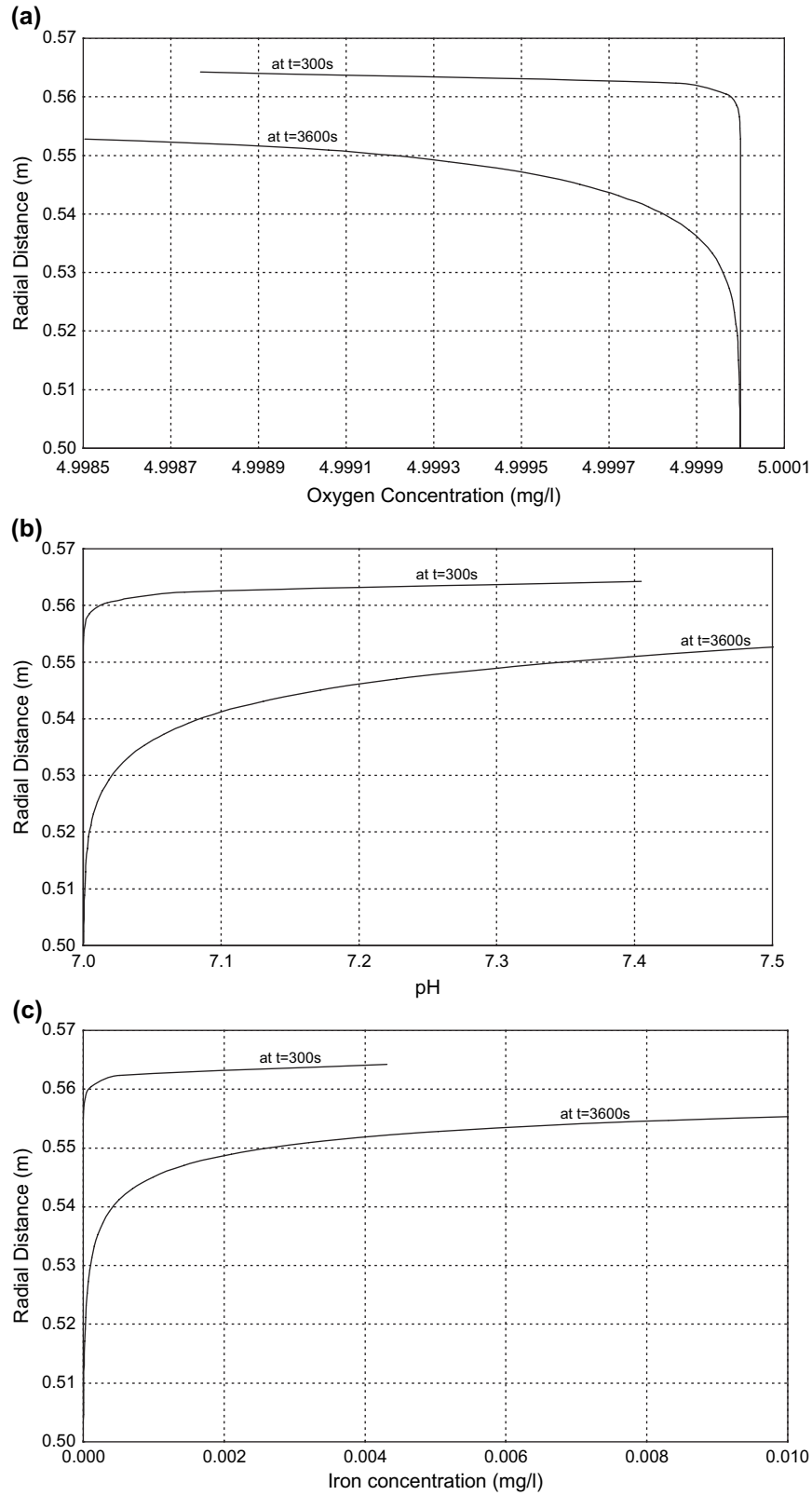


Fig. 5. Concentration along the section; (a) DO concentration, (b) pH, (c) iron release.

is a reasonable consistency between the 1-D and 2-D results and both models predict the same pattern for chemical concentrations. The slight difference between the 1-D and 2-D models can be attributed to the effect of the velocity profile.

Considering the no-slip condition at pipe wall, Eq. (13) shows that diffusion is the only mechanism for transport oxygen from bulk flow into the pipe wall in 2-D model; whereas both diffusion and advection are responsible for the 1-D case.

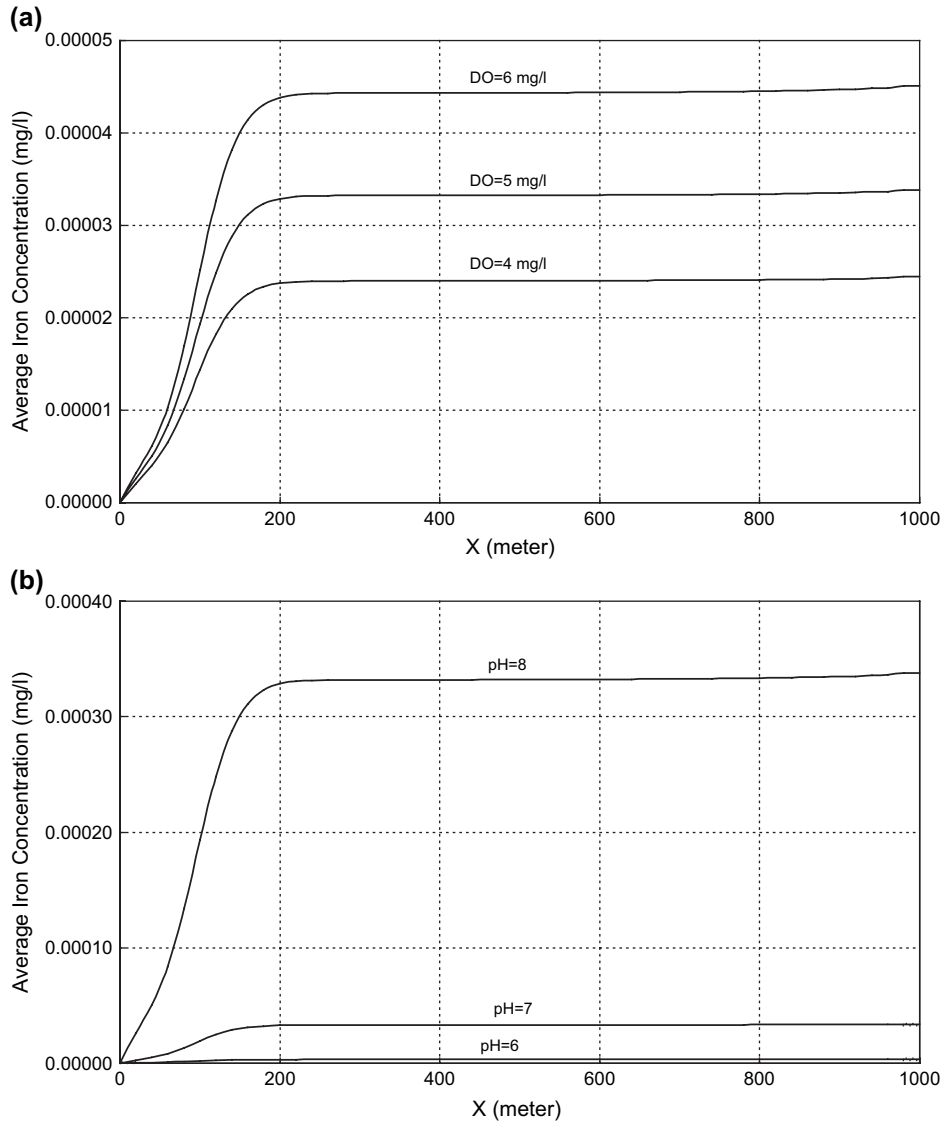


Fig. 6. Effect of initial conditions on iron release 300 s after start-up; (a) initial DO concentration and (b) initial pH.

Although the results show that oxygen concentration is steadily decreasing in time, and therefore iron release and pH are increasing. In practice the corrosion rate is also influenced not only by the so-called secondary reactions but also by many other reactions (e.g., disinfectant decay) or even microorganisms (Lee et al., 1980). The current study focuses on the primary reactions only. Yet, even here, there is a thermodynamic limitation in actual systems as the chemical concentration approaches the equilibrium state. For example, Eq. (8) effectively limits the maximum concentration of ferrous ion and other such equilibrium constraints may limit corrosion rates in real systems. Chemical equilibrium does not occur within the short time period of the current study.

The iron release rate is locally investigated through the study of increase/decrease in DO concentration, solution pH, and iron concentration at midpoint of the pipe. The results for the 2-D simulation are shown graphically in Fig. 5a–c for radial distribution of DO concentration, pH, and iron

release 300 and 3600 s after the valve start-up, respectively. The figures clearly show that the ion species react in the vicinity of the pipe wall and then diffuse outward. Fig. 5b particularly shows a significant difference (more than one in pH unit) between the pH at the pipe wall and the pipe centerline. The high pH near the pipe wall can strongly affect the secondary reactions, and thus, the corrosion rate. Measured differences between the solution pH at the pipe wall and that at the pipe centerline may be three to even four in pH units (AWWARF, 1996) highlighting a possible advantage of the 2-D simulation.

6.1. Effect of initial concentration of chemicals

Since DO is often a dominant oxidant, the effect of initial concentration of DO on iron release is investigated and the results (300 s after start-up) are given in Fig. 6a for the 2-D simulation model. Interestingly, the simulation shows the increase in iron concentration with increase in initial DO concentration.

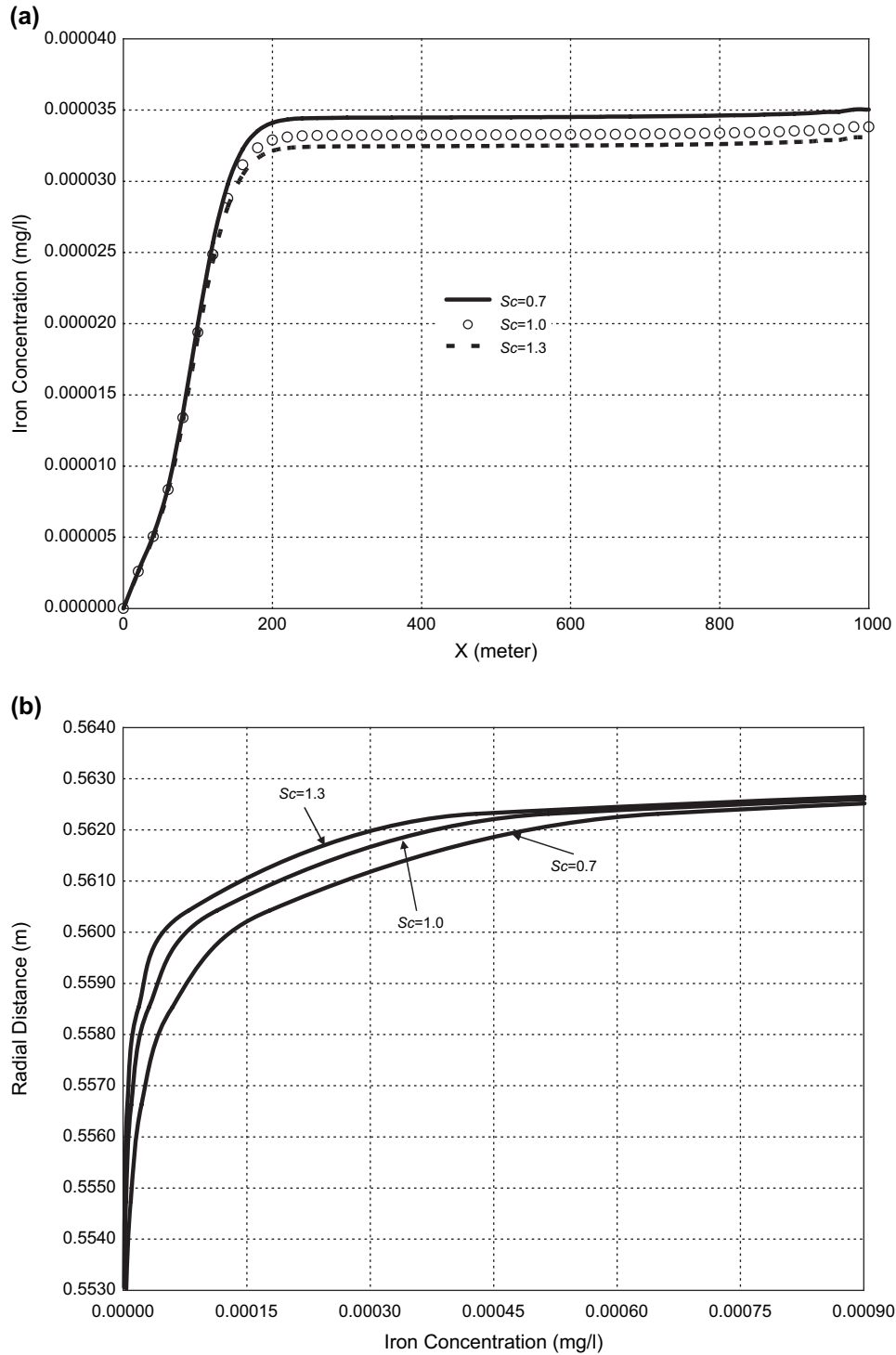


Fig. 7. Effect of Schmidt number on iron release 300 s after start-up; (a) along the pipe and (b) along a section at the middle of the pipe.

It should be emphasized that although the initial concentration has a significant influence on corrosion rate in a new WDS, it is less significant in old systems, due to the presence of scales and tubercles at the pipe wall of an old WDS, the transfer mechanism of oxygen from the bulk flow into the pipe wall. In fact, in an old WDS with no flow (stagnation period), the corrosion may decrease with increasing DO concentration (Sarin et al., 2001). A follow-up study might more carefully consider this issue.

Due to the importance of pH as a key parameter, a numerical study is conducted for the effect of initial pH on the iron release and the results of the 2-D simulation model are plotted in Fig. 6b at 300 s after start-up. As is clear from the figure, the initial pH has a strong influence on the ferrous ion concentration. Thus, for two similar systems with the same hydraulic and initial DO concentration but different initial pH, the system with higher initial pH would have higher iron release. This dependency between pH and corrosion

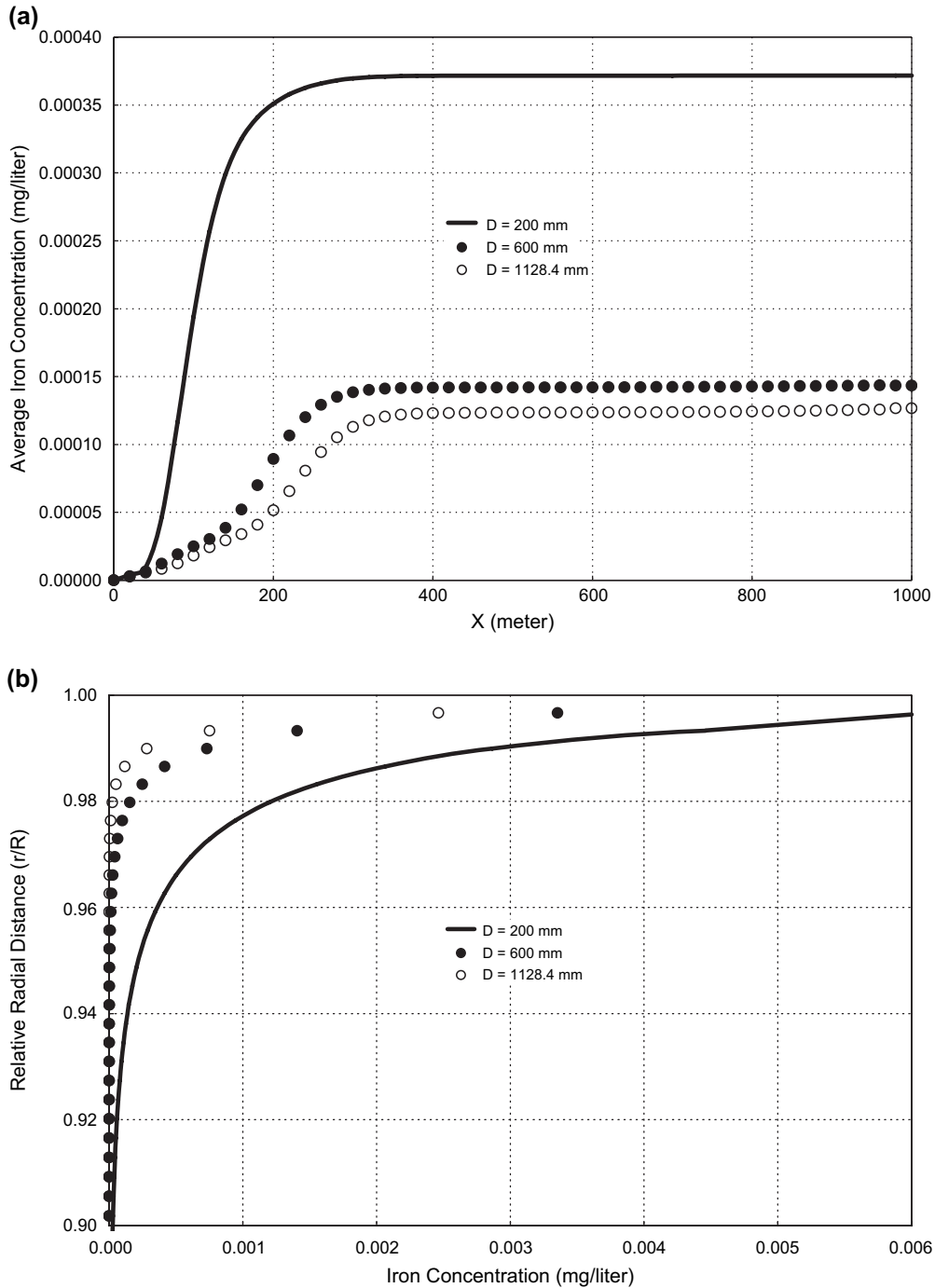


Fig. 8. Effect of pipe diameter on iron release 300 s after start-up; (a) along the pipe length and (b) in radial direction.

rate is more obvious from Eq. (10). For a system with no flow (stagnant water), Eq. (10) shows a higher corrosion rate if the system has higher hydroxide ion (OH^-) concentration (and therefore higher pH). This finding is consistent with the literature as well. In practice, although the high concentration of H^+ ion in the water at lower pH can potentially behave as an additional oxidant and therefore increase the corrosion rate, the decrease in buffer capacity and also the formation of non-protective scales can also lead to a higher corrosion at higher pH.

6.2. Effect of Schmidt number and diffusion

As mentioned, the turbulent Schmidt number is the ratio of the eddy viscosity to the diffusivity of the scalar constituent. Using the Reynolds analogy, it turns out that the turbulent Schmidt number is around unity (Rubin and Atkinson, 2001). A sensitivity analysis was conducted to investigate the effectiveness of this number on the model results. Fig. 7 demonstrates the results of this analysis for the 2-D model. More clearly, Fig. 7a shows the effect of Schmidt number

on iron release (into the bulk flow) along the pipe 300 s after the start-up through the changes in the Schmidt number from 0.7 to 1.3. Although they are dramatic, the figure indicates relatively noticeable differences in iron concentration due to changes in the Schmidt number. In fact, decreasing the Schmidt number increases the diffusion of oxygen from the bulk flow into the pipe wall region, and consequently increases the corrosion rate. This is more obvious through the detailed comparison between the iron concentration plots in radial direction (at a section in the middle of the pipe) for different turbulent Schmidt numbers given in Fig. 7b. Interestingly, however, the figure clearly shows more iron diffusion along the section by decreasing the Schmidt number. This highlights the fact that although advection dominates in the particular case considered in this study, and even in most real systems, the availability of oxygen (or any other oxidant) at the pipe wall also influences corrosion. In fact, diffusion progressively dominates mass transport as one approaches a “no flow” condition, such as in a dead end segment.

6.3. Effect of pipe diameter and flow velocity

Several simulations were performed for different other case studies to investigate the effects of the pipe diameter on the iron release. Considering the flow velocity 1.6 m/s for all cases, the results of the 2-D model are plotted in Fig. 8a, b for iron concentration (300 s after the start-up) along the pipe length and a cross-section located at the middle of the pipe. Interestingly, both figures show an increase in iron release by a decrease in pipe diameter. In other words, the study indicated that fairly high iron concentration can accumulate in the water in smaller pipes. This is consistent with the findings of many water utilities that consumer complaints regarding rusty water are usually from the locations with the smaller-diameter pipes (AWWARF, 1996). Clearly iron release rate does not have a linear relationship with the pipe diameter: the change in release rate from 1128.4 mm to 600 mm pipe is much smaller than that from 600 mm to 200 mm pipe. This is likely a consequence of the stronger influence of diffusion in smaller-diameter pipes.

A sensitivity analysis was conducted on the effect of velocity on iron release. The analysis shows a decrease in release rate with an increase in velocity. This largely reflects the role of residence time, which is higher for systems with lower velocity. For this reason, velocity by itself is an insufficient basis for comparing corrosion results under different hydraulic conditions. Other factors such as velocity profile, wall shear stresses, and residence time should also be considered. This is generally in agreement with findings by Pisigan and Singley (1987) that the corrosion rate is higher at low Reynolds numbers. However, there is also literature support for a higher iron release with increasing velocity (Fang and Liu, 2003), highlighting the fact that the increase in corrosion rate can more than compensate for the reduction in contact time, strongly hinting at the importance of accelerated turbulent exchange with the wall.

7. Practical utility of the 1-D and 2-D models

The numerical studies of the reservoir-pipe-valve-reservoir case in this research required approximately 3 weeks to perform the proposed 2-D simulation approach over a DELL INSPIRON-8200 Pentium 4 laptop (1.8 GHz); the corresponding simulation time for the 1-D approach is of the order of an hour when a consistent numerical grid size is used. The long simulation time makes the application of the proposed 2-D approach questionable in practice when several chemical and biochemical reactions affect the pipe corrosion, particularly for large systems and longer simulation times.

Moreover, to be useful, numerical methods must be convergent and stable. Karney and Ghidaoui (1997) confirmed that the Courant condition ($Cr = a\Delta t/\Delta x \leq 1.0$) is indeed necessary to assure a stable numerical solution for the hyperbolic equations of continuity and momentum. This reality affects the WQ model through the numerical-cell advective numbers ($\Delta t/\Delta x$ and $\Delta t/\Delta r$), Peclet numbers ($U\Delta t/\Delta x$ and $V\Delta t/\Delta r$), and diffusion numbers ($v_i\Delta t/\Delta x^2$ and $v_i\Delta t/\Delta r^2$) appearing in Eqs. (11) and (12). It has been provisionally verified by Ferziger (1981) that, although each individual differenced equation from one time level (n) to the next ($n + 1$); namely Eqs. (11) and (12), is conditionally stable, the two-step ADI algorithm is a stable technique when applied to parabolic PDEs with constant coefficients, whereas in the case of transient-flow problems the coefficients change in both time and space. Therefore, the stability criterion clearly depends on the nature of the transient flow and the reaction rate terms. Hence, more study is required to refine and clarify the criterion. Although the stability could not be extensively studied for the multicomponent model, and relatively long simulation time for the 2-D model, a number of runs for the single component scenario were conducted to investigate the effects of the mesh size (in both radial and longitudinal directions) on the numerical convergence. The results showed that the proposed 2-D model becomes progressively more accurate as a finer numerical mesh was chosen. However, simulation time was dramatically increased as a finer numerical mesh was chosen.

8. Conclusion

A WDS is a dynamically complicated system in which different physical, chemical, and microbiological events may occur simultaneously resulting in the change in the quality of water. Indeed, multicomponent processes in general and corrosion in particular are complex problems owing to the variety and number of reactions and transport mechanisms occurring in the system. These processes have traditionally been studied through experimental correlations and few serious computer simulations have considered the effects of both hydraulic and chemical issues on the corrosion. This preliminary study determines the concentration of chemicals released into the bulk flow through a bulk water and pipe wall reactions.

Although the study showed an overall consistency between the 1-D and 2-D results and both models predict the same pattern for chemical concentrations, there exists a noticeable difference between the two sets of results, which can be associated to the significant role of the velocity profile in 2-D model.

Considering oxidation–reduction reaction as the prime mechanism for pipe wall corrosion, the results showed that DO is steadily decreasing (and therefore iron release and pH of the solution are increasing) with time. In practice, however, the corrosion rate is also influenced by other chemicals within the flow via the so-called secondary and tertiary reactions and even via biological activities by microorganisms. These should be studied in a more comprehensive research in future. The study highlighted the significant influence of DO and pH of the solution on the iron release rate: systems with higher initial DO-concentrations or pH would have higher iron release. However, regarding their impacts, the study shows that the initial DO concentration has less effect on the iron release than initial pH does. Yet there is great need for the publication of detailed experiment data sets to allow full evaluation of such transient water quality models.

The study indicates a fairly high accumulation of iron concentration in the water due to a decrease in pipe-diameter or an increase in the flow velocity. Generally, the study shows that although there is qualitatively an overall agreement between the 1-D and 2-D models, 2-D models have considerable additional potential that cannot be realized through 1-D approach.

Acknowledgment

This research was financed in part by the grants from the University of Toronto and the Canadian Water Network. The support is gratefully acknowledged.

Appendix

Using the central finite difference discretization scheme, the coefficients in Eqs. (11) and (12) were derived as follows (the subscripts i and j denote the position of the node in longitudinal and radial directions, respectively and the superscript n denotes the time level):

- Intermediate time level $n + 1/2$: the scheme is implicit in radial direction but explicit in longitudinal direction, hence:

$$A_1 = \frac{1}{\bar{r}_{j+1} - \bar{r}_{j-1}} V_{ij}^{n+1/2} - \alpha_1 \quad (16)$$

$$B_1 = \frac{2}{\Delta t} - \beta_1 \quad (17)$$

$$E_1 = \frac{-1}{\bar{r}_{j+1} - \bar{r}_{j-1}} V_{ij}^{n+1/2} - \gamma_1 \quad (18)$$

$$F_1 = \left[\frac{-U_{ij}^n}{\Delta x} + \alpha_2 \right] C_{k_{i+1,j}}^n + \left[\frac{2}{\Delta t} + \beta_2 \right] C_{k_{i,j}}^n + \left[\frac{U_{ij}^n}{\Delta x} + \gamma_2 \right] C_{k_{i-1,j}}^n \quad (19)$$

$$\alpha_1 = \frac{1}{\bar{r}_j(\bar{r}_{j+1} - \bar{r}_j)} \left[\frac{\bar{r}_{j+1}}{\bar{r}_{j+1} - \bar{r}_j} \Gamma_{k_{i,j+1/2}}^{n+1/2} \right] \quad (20)$$

$$\gamma_1 = \frac{1}{\bar{r}_j(\bar{r}_{j+1} - \bar{r}_j)} \left[\frac{\bar{r}_j}{\bar{r}_j - \bar{r}_{j-1}} \Gamma_{k_{i,j-1/2}}^{n+1/2} \right] \quad (21)$$

$$\beta_1 = -(\alpha_1 + \gamma_1) \quad (22)$$

$$\alpha_2 = \frac{1}{\Delta x^2} \Gamma_{k_{i+1/2,j}}^n \quad (23)$$

$$\gamma_2 = \frac{1}{\Delta x^2} \Gamma_{k_{i-1/2,j}}^n \quad (24)$$

$$\beta_2 = -(\alpha_2 + \gamma_2) \quad (25)$$

- Advanced time level $n + 1$: the scheme is explicit in radial direction but implicit in longitudinal direction, hence:

$$A_2 = \frac{U_{ij}^{n+1}}{\Delta x} - \alpha_4 \quad (26)$$

$$B_2 = \frac{2}{\Delta t} - \beta_4 \quad (27)$$

$$E_2 = \frac{-U_{ij}^{n+1}}{\Delta x} - \gamma_4 \quad (28)$$

$$F_2 = \left[\frac{-V_{ij}^{n+1/2}}{\bar{r}_{j+1} - \bar{r}_{j-1}} + \alpha_3 \right] C_{k_{i,j+1}}^{n+1/2} + \left[\frac{2}{\Delta t} + \beta_3 \right] C_{k_{i,j}}^{n+1/2} + \left[\frac{V_{ij}^{n+1/2}}{\bar{r}_{j+1} - \bar{r}_{j-1}} + \gamma_3 \right] C_{k_{i,j-1}}^{n+1/2} \quad (29)$$

$$\alpha_3 = \frac{1}{\bar{r}_j(\bar{r}_{j+1} - \bar{r}_j)} \left[\frac{\bar{r}_{j+1}}{\bar{r}_{j+1} - \bar{r}_j} \Gamma_{k_{i,j+1/2}}^{n+1/2} \right] \quad (30)$$

$$\gamma_3 = \frac{1}{\bar{r}_j(\bar{r}_{j+1} - \bar{r}_j)} \left[\frac{\bar{r}_j}{\bar{r}_j - \bar{r}_{j-1}} \Gamma_{k_{i,j-1/2}}^{n+1/2} \right] \quad (31)$$

$$\beta_3 = -(\alpha_3 + \gamma_3) \quad (32)$$

$$\alpha_4 = \frac{1}{\Delta x^2} \Gamma_{k_{i+1/2,j}}^{n+1} \quad (33)$$

$$\gamma_4 = \frac{1}{\Delta x^2} \Gamma_{k_{i-1/2,j}}^{n+1} \quad (34)$$

$$\beta_4 = -(\alpha_4 + \gamma_4) \quad (35)$$

in which Δt , Δx are the time step and the length of each reach in longitudinal direction. The term \bar{r} is defined as following:

$$\bar{r}_j = (r_j + r_{j-1})/2 \quad (36)$$

The subscript k in Eqs. (16)–(35) denotes the chemical constituents in the water.

References

- Abbott, M.B., Minns, A.W., 1998. Computational Hydraulics, second ed. Brookfield/Andershot, VT/England.
- Anon., 1878. Amtsblatt des Koniglich Wurttembergischen Ministeriums des Inneren, Stuttgart, No. 7, pp. 101–106.
- AWWARF, 1996. Internal Corrosion of Water Distribution Systems, second ed. American Water Works Association Research Foundation, Denver, USA.
- Benefield, L.D., Judkins, J.F., Weand, B.L., 1982. Process Chemistry for Water and Wastewater Treatment. Prentice-Hall Inc., USA.
- Boulos, P., Altman, T., Bowcock, R., Dhingra, A., Collevati, F., 1993. An explicit algorithm for modeling distribution system WQ with applications. In: Miller, D.S. (Ed.), Second BHR International Conference on Water Pipeline Systems, Edinburgh, Scotland. Mechanical Publications Limited, London, pp. 405–432.
- Boulos, P., Altman, T., Jarriage, P., Collevati, F., 1995. Discrete simulation approach for network WQ models. Journal of Water Resources Planning and Management 121 (1), 49–60.
- Clark, R., Grayman, W., Males, R., 1988. Contaminant propagation in distribution system. Journal of Environmental Engineering, ASCE 114 (4), 929–943.
- De Mussy, 1849. *Dubl. Q. Jl. Med. Sci.*, May.
- Fang, C.S., Liu, B., 2003. Hydrodynamic and temperature effects on the flow-induced local corrosion in pipelines. In: Chemical Engineering Communication, vol. 190. Taylor and Francis. 1249–1266.
- Fernandes, C., Karney, B.W., 2004. Modeling the advection equation under water hammer conditions. Urban Water Journal, Special Issue on Transient 1 (2), 97–112.
- Ferziger, J.H., 1981. Numerical Methods for Engineering Application. Wiley, New York.
- Grayman, W., Clark, R., Males, R., 1988. Modeling distribution WQ: dynamic approach. Journal of Water Resources Planning and Management 114 (3), 295–312.
- Karney, B.W., Ghidaoui, M.S., 1997. Flexible discretization algorithm for fixed-grid MOC in pipelines. Journal of Hydraulic Engineering 123, 1004–1011.
- Kita, Y., Adachi, Y., Hirose, K., 1975. Periodically oscillating turbulent flow in a pipe. Bulletin of the JSME 23 (179), 656–664.
- Kuch, A., Wagner, I., 1983. A Mass Transfer Model to Describe Lead Concentration in Drinking Water. Water Resources 17 (8), 1303–1307.
- Lee, S.H., O'Connor, J.T., Banerji, S.K., 1980. Biologically mediated corrosion and its effects on WQ in distribution systems. Journal of the American Water Works Association 72, 636.
- Liou, C., Kroon, J., 1987. Modeling the propagation of waterborne substance in distribution networks. Journal of the American Water Works Association 79 (11), 54–58.
- Ozdemir, O.N., Ger, A.M., 1998. Realistic numerical simulation of chlorine decay in pipes. Water Research 32 (11), 3307–3312.
- Ozdemir, O.N., Ger, A.M., 1999. Unsteady 2-D chlorine transport in water supply pipes. Water Research 33 (17), 3637–3645.
- Pisigan, R.A., Singley, E., 1987. Influence of buffer capacity chlorine residual and flow rate on corrosion of mild steel and copper. Journal of the American Water Works Association 79 (2), 67–70.
- Rodi, W., 1993. Turbulence Models and Their Application in Hydraulics: A State of the Art Review, third ed. A.A. Balkema, Rotterdam, Netherlands.
- Rossmann, L., Boulos, P., Altman, T., 1993. Discrete volume-element method network water quality models. Journal of Water Resources Planning and Management 119 (5), 505–517.
- Rossmann, L., Boulos, P., 1996. Numerical methods for modeling WQ in distribution systems: a comparison. Journal of Water Resources Planning and Management 122 (2), 137–146.
- Rubin, H., Atkinson, J., 2001. Environmental Fluid Mechanics. Marcel Dekker Inc., USA.
- Sarin, P., Snoeyink, V.L., Bebee, J., Kriven, W.M., Clement, J.A., 2001. Physico-chemical characteristics of corrosion scales in old iron pipes. Water Research 35 (10), 2961–2969.
- Tanggara, A., 2004. Preliminary Model of Corrosion and Iron Release in a Pipeline System. An M.Sc. thesis presented to the Civil Engineering Department, University of Toronto, Toronto, Canada.
- Vardy, E., Hwang, K.L., 1991. A characteristic model of transient friction in pipes. Journal of Hydraulic Research 29 (5), 669–684.
- Waanders, B.G.B., Shadid, J., Collis, S., Hammond, G.G., Murray, R., 2005. A comparison of Navier Stokes and network models to predict chemical transport in municipal water distribution systems. In: Seventh Annual Symposium on Water Distribution Systems Analysis, World Water and Environmental Resources Congress, EWRI, Anchorage, Alaska, USA, May 15–19.
- Wood, D.J., 1980. Slurry flow in pipe networks. Journal of Hydraulic Engineering, ASCE 106 (1), 57–70.
- Zhao, M., Ghidaoui, M.S., 2003. An efficient solution for quasi two-dimensional water hammer problems. Journal of Hydraulic Engineering, ASCE 129 (10), 1007–1013.